

Article

Asymptotic Analysis of an Elastic Layer under Light Fluid Loading

Sheeru Shamsi  and Ludmila Prikazchikova * 

School of Computer Science and Mathematics, Keele University, Keele ST5 5BG, UK; s.s.shamsi@keele.ac.uk

* Correspondence: l.prikazchikova@keele.ac.uk

Abstract: Asymptotic analysis for an elastic layer under light fluid loading was developed. The ratio of fluid and solid densities was chosen as the main small parameter determining a novel scaling. The leading- and next-order approximations were derived from the full dispersion relation corresponding to long-wave, low-frequency, antisymmetric motions. The asymptotic plate models, including the equations of motion and the impenetrability condition, motivated by the aforementioned shortened dispersion equations, were derived for a plane-strain setup. The key findings included, in particular, the necessity of taking into account transverse plate inertia at the leading order, which is not the case for heavy fluid loading. In addition, the transverse shear deformation, rotation inertia, and a number of other corrections appeared at the next order, contrary to the previous asymptotic developments for fluid-loaded plates not assuming a light fluid loading scenario.

Keywords: fluid–structure interaction; elastic layer; asymptotic analysis; light fluid loading; refined plate models

MSC: 74F10

Citation: Shamsi, S.; Prikazchikova, L. Asymptotic Analysis of an Elastic Layer under Light Fluid Loading. *Mathematics* **2024**, *12*, 1465. <https://doi.org/10.3390/math12101465>

Academic Editor: Marco Pedroni

Received: 30 March 2024

Revised: 29 April 2024

Accepted: 6 May 2024

Published: 9 May 2024



Copyright: © 2024 by the authors. Licensee MDPI, Basel, Switzerland. This article is an open access article distributed under the terms and conditions of the Creative Commons Attribution (CC BY) license (<https://creativecommons.org/licenses/by/4.0/>).

1. Introduction

Numerous problems involving vibrating structures under fluid loading have been studied in the literature since the late nineteenth century; for example, see “Theory of Sound” [1] by Lord Rayleigh. The theoretical analysis on the subject most often makes use of 2D structural theories such as the classical Kirchhoff theory for thin elastic plates, e.g., see the 1988 Rayleigh medal lecture [2] and the books [3,4]. Ideally, approximate coupled models in fluid–structure interaction have to be mathematically justified starting from 3D dynamic theory in linear elasticity. At the same time, until recently, there have been limited attempts to address this matter, mainly using the traditional formulations based on 2D engineering structural theories using analytical methods [5–9], as well as [10–14] promoting experimental and numerical techniques. As an exception, we mention the paper by Johansson et al. [15], attempting to address this problem in the context of a fluid-loaded elastic plate but lacking an asymptotic consistency. We also mention a previous effort to adapt refined asymptotic setups for thin elastic shells not in contact with fluid to fluid–structure interaction problems; e.g., see [16]. A fresh work by Kaplunov et al. [17] developed a hierarchy of asymptotic models for a fluid-loaded elastic layer, emphasising the point that such a layer requires a special treatment, extending the well-established setup of Neumann boundary conditions for a layer with traction-free or mechanically loaded faces; e.g., see [18]. In this case, the effect of fluid loading supports the so-called fluid-borne bending wave; e.g., see [19], which assumed a novel asymptotic scaling. The methodology developed in [17] was next extended to low-frequency acoustic wave scattering by a circular cylindrical shell in [20].

It is worth noting that the aforementioned scaling does not cover the important scenario of light fluid loading, for which the ratio of the density of the fluid to the density of the solid is small. The general understanding of the related asymptotic limit from the prospects of dynamic elasticity seems to be of significant interest for modelling various

fluid-loaded elastic structures. A special focus on the light fluid loading limit is given by Craster [21], establishing a perturbation scheme to obtain a robust approximate solution for a fluid-loaded elastic solid; see also [22,23], tackling both light and heavy fluid loading limits. A detailed asymptotic analysis of a Kirchhoff plate under light fluid loading was reported by Chapman and Sorokin [24] using the same small parameter as in the cited paper [21], involving the product of not only the ratio of densities of fluid and plate, but also the related wave speeds. The aforementioned small parameter was also adopted in [25], dealing with acoustic radiation due to harmonic vibrations of an elastic layer over a broad frequency range.

The proposed analysis is motivated by a lack of consistent fluid-structure models taking into account the effect of fluid loading. In particular, the dimension reduction for immersed thin-walled structures has not been yet asymptotically validated. To this end, the considerations in [17,20] have to be extended to the case of light fluid loading.

As an example, in this paper, we study a plane-strain time-harmonic problem for an elastic layer immersed into compressible fluid. The ratio of densities is chosen as the main small parameter. It seems to be more appropriate for the considered framework than that adopted in [21,24]. Below, for the sake of simplicity, we determine the long-wave scale through the above-mentioned small parameter. Its presence affects the asymptotic analysis of fluid-borne wave dictation taking into account the plate transverse inertia at the leading order. The transverse shear deformation, rotation inertia, and similar corrections, including those in the impenetrability condition, also appear at lower-order approximations in comparison with the treatment in paper [17].

This paper is organised as follows. The governing equations are given in Section 2. Section 3 is concerned with the derivation of the leading and first-order approximations to the full dispersion relation over the low-frequency range in the light fluid loading limit. This motivates the scaling for further asymptotic analysis of the problem. Section 4 aims at the formulation of the asymptotic models, supporting the above-mentioned approximations of the dispersion relation. The presentation in this section is structured similar to that in [17], which does not assume light fluid loading. The concluding remarks are summarised in Section 5.

2. Governing Equations

Consider small-amplitude free vibrations of an isotropic linearly elastic layer of thickness $2h$ immersed in a non-viscous compressible fluid. The Cartesian coordinate system is set up in such a way that axis x_1 goes through the midplane of the layer; see Figure 1. The axis x_2 , perpendicular to the plane (x_1, x_3) , is not shown in the figure. The following notation is used throughout the paper: E is Young's modulus, ν is the Poisson's ratio, ρ and ρ_0 are the solid and fluid densities, respectively, c_0 is the wave speed in fluid, and $c_2 = \sqrt{E/2\rho(1+\nu)}$ is the shear wave speed in solid.

We limit ourselves to a plane-strain problem in the coordinates (x_1, x_3) . Thus, the equations of motion in linear elasticity may be written as

$$\begin{aligned}\frac{\partial\sigma_{11}}{\partial x_1} + \frac{\partial\sigma_{31}}{\partial x_3} - \rho\frac{\partial^2 v_1}{\partial t^2} &= 0, \\ \frac{\partial\sigma_{13}}{\partial x_1} + \frac{\partial\sigma_{33}}{\partial x_3} - \rho\frac{\partial^2 v_3}{\partial t^2} &= 0.\end{aligned}\tag{1}$$

Here and below, v_k ($k = 1, 3$) are displacements, σ_{mn} ($m, n = 1, 2, 3$) are stresses, and t denotes time. The stresses and displacements given in the above equations satisfy the following relations, e.g., see [18]

$$\begin{aligned}
 \sigma_{11} &= \frac{E}{1-\nu^2} \frac{\partial v_1}{\partial x_1} + \frac{\nu}{1-\nu} \sigma_{33}, \\
 \sigma_{22} &= \frac{E\nu}{1-\nu^2} \frac{\partial v_1}{\partial x_1} + \frac{\nu}{1-\nu} \sigma_{33}, \\
 \frac{\partial v_3}{\partial x_3} &= \frac{1}{E} \left(\sigma_{33} - \nu(\sigma_{11} + \sigma_{22}) \right), \\
 \frac{\partial v_1}{\partial x_3} &= -\frac{\partial v_3}{\partial x_1} + \frac{2(1+\nu)}{E} \sigma_{31},
 \end{aligned}
 \tag{2}$$

adapted for the forthcoming asymptotic analysis.

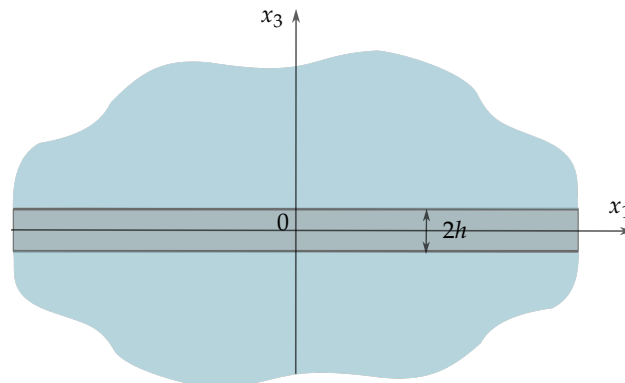


Figure 1. Elastic layer immersed in fluid.

In addition, the fluid velocity potential $\varphi(x_1, x_3, t)$, see for example [25–27], satisfies the wave equation

$$\frac{\partial^2 \varphi}{\partial x_1^2} + \frac{\partial^2 \varphi}{\partial x_3^2} - \frac{1}{c_0^2} \frac{\partial^2 \varphi}{\partial t^2} = 0,
 \tag{3}$$

with the interfacial conditions at $x_3 = \pm h$, given by

$$\sigma_{31} = 0, \quad \sigma_{33} = \rho_0 \frac{\partial^2 \varphi}{\partial t^2}, \quad v_3 = \frac{\partial \varphi}{\partial x_3}.
 \tag{4}$$

The main objective of this paper is to derive asymptotic models of the formulated problem over a long-wave low-frequency region under the conditions of light fluid loading. For this, $\rho_0 \ll \rho$, and $h \ll L$ and $h/c_2 \ll T$, with L and T denoting a typical wavelength and time scale, respectively. We also restrict ourselves to bending vibrations. Prior to proceeding with the asymptotic treatment of the equations of motion, we first study the associated shortened forms of the dispersion relation corresponding to (1)–(4).

3. Asymptotic Analysis of the Dispersion Relation

In this section, we analyse the antisymmetric dispersion relation, e.g., see [28]

$$\Omega^4 r \cosh(A) \cosh(B) + H \left((2K^2 - \Omega^2)^2 \frac{\sinh(A)}{A} \cosh(B) - 4K^2 B^2 \frac{\sinh(B)}{B} \cosh(A) \right) = 0,
 \tag{5}$$

with

$$A = \sqrt{K^2 - \Omega^2 \kappa^2}, \quad B = \sqrt{K^2 - \Omega^2}, \quad H = \sqrt{K^2 - \Omega^2 \delta^2},
 \tag{6}$$

and

$$\Omega = \frac{\omega h}{c_2}, \quad K = kh,
 \tag{7}$$

where ω and k are angular frequency and wavenumber, respectively; $\delta = \frac{c_2}{c_0}$ and $\kappa = \sqrt{\frac{1-2\nu}{2-2\nu}}$.

Let us assume that $r = \rho_0/\rho \ll 1$ for a light fluid loading scenario and try the long-wave low-frequency scaling

$$\Omega = \Omega_* r^2, \quad K = K_* r, \tag{8}$$

where Ω_* and K_* are assumed so far to be of order unity. In this case, the relation $\Omega \sim K^2$, characteristic of the bending wave on a free elastic plate, is satisfied; e.g., see [18].

Expanding Equation (5) into a Taylor series and taking into account the scaling (8), we obtain a two-term expansion in the small parameter, r ,

$$\begin{aligned} & \left((K_* + 1)\Omega_*^2 + \frac{2K_*^5}{3(\nu - 1)} \right) \\ & + \frac{(-15\delta^2(\nu - 1)\Omega_*^4 + ((-10\delta^2 + 20(\nu - 2))K_* + 30(\nu - 1))K_*^3\Omega_*^2 + 4K_*^8)}{30K_*(\nu - 1)} r^2 = 0. \end{aligned} \tag{9}$$

At the leading order, it yields

$$\Omega_*^2 = \frac{2K_*^5}{3(K_* + 1)(1 - \nu)}. \tag{10}$$

Now, by replacing the Ω_*^2 and Ω_*^4 terms in the coefficient at r^2 in (9) using (10), we obtain an $O(r^2)$ correction to the leading-order estimation. It takes the form of

$$\Omega_*^2 = \frac{2K_*^5}{3(K_* + 1)(1 - \nu)} + \frac{2((7\nu - 17)K_*^2 - (5\delta^2 - 19\nu + 29)K_* + 12(\nu - 1))K_*^7}{45(K_* + 1)^3(1 - \nu)^2} r^2. \tag{11}$$

Next, consider two limiting behaviours, for which $K_* \ll 1$ and $K_* \gg 1$, in order to elucidate the relation with previous results. For the first case, we obtain from (10) and (11)

$$\Omega_*^2 = \frac{2K_*^5}{3(1 - \nu)}, \tag{12}$$

and

$$\Omega_*^2 = \frac{2K_*^5}{3(1 - \nu)} - \frac{2K_*^6}{3(1 - \nu)}, \tag{13}$$

respectively. In terms of parameters K and Ω , the latter becomes

$$\Omega^2 = \frac{2K^5}{3r(1 - \nu)} - \frac{2K^6}{3r^2(1 - \nu)}. \tag{14}$$

It is worth noting that it is identical to the two-term expansion in [28], not assuming light fluid loading.

For $K_* \gg 1$ we have from (10) and (11)

$$\Omega_*^2 = \frac{2K_*^4}{3(1 - \nu)}, \tag{15}$$

and

$$\Omega_*^2 = \frac{2K_*^4}{3(1 - \nu)} + \frac{2(7\nu - 17)r^2K_*^6}{45(1 - \nu)^2}. \tag{16}$$

We remark that for a plate without fluid loading, the two-term expansion of the Rayleigh–Lamb dispersion relation for the bending wave in the long-wave low-frequency region ($\Omega \sim K^2, K \ll 1$) is given by, see [18],

$$\Omega^2 = \frac{2K^4}{3(1-\nu)} + \frac{2(7\nu-17)K^6}{45(1-\nu)^2}. \tag{17}$$

The last formula, rewritten in terms of K_* and Ω_* , coincides with (16).

The rest of this section reports on numerical results for a steel layer immersed in water, illustrated by Figures 2 and 3. The graphs presented in this paper have been produced using Python and Maple 2021 software. The problem parameters utilised are $c_0 = 1480 \text{ m s}^{-1}$, $\nu = 0.2$, $c_2 = 3156 \text{ ms}^{-1}$, $\rho = 7800 \text{ kgm}^{-3}$, and $\rho_0 = 1000 \text{ kgm}^{-3}$. Hence, the small parameter, characteristic of the light fluid loading, is $r = \rho_0/\rho \approx 0.128$. Indeed, this type of small parameter could be relevant to other materials, not just a steel/water combination. The latter is chosen in this paper to illustrate the behaviour corresponding to light fluid loading. For other materials with the same parameter r , the graphs will look similar.

The dispersion curves for leading-order (10) and first-order (11) approximations are shown in Figure 2, along with that for the full dispersion relation (5), rewritten in terms of (8). As can be observed, the first-order approximation works better in comparison with the leading order one due to the fact that it takes into account higher-order terms in the expansions and hence is in better agreement with the full dispersion relation.

Figure 3 demonstrates the limiting cases $K_* \ll 1$ and $K_* \gg 1$ of the leading-order approximation (10). It shows the comparison of the leading-order approximation (10) with the one-term expansions (12) and (15), oriented to the regions $K_* \ll 1$ and $K_* \gg 1$, respectively. The intersection of the blue and red curves in Figure 3 arises due to the approximation error being equal for both dispersion curves.

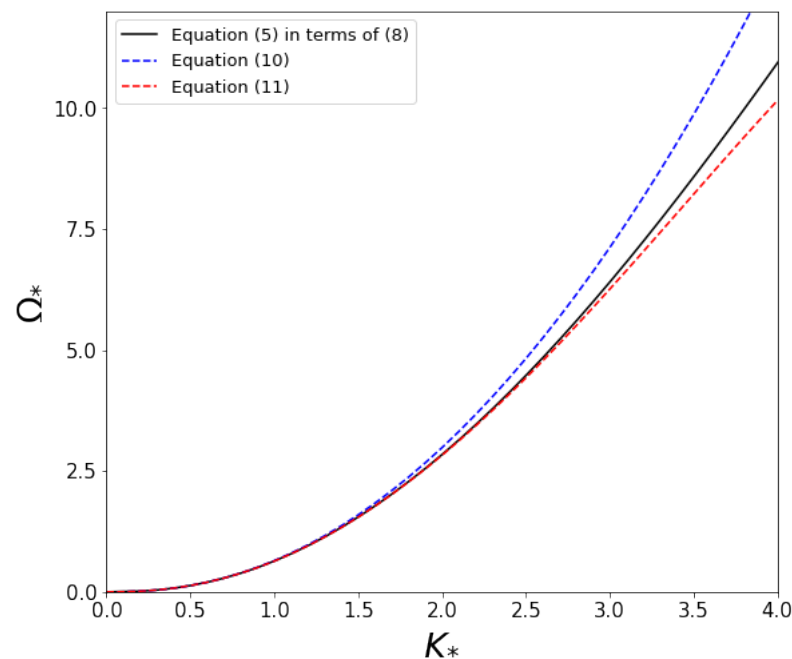


Figure 2. Comparison of the exact (solid black line) dispersion relation ((5) rewritten in terms of (8)) with the leading order-approximation (10) (dashed blue line) and the first-order approximation (11) (dashed red line).

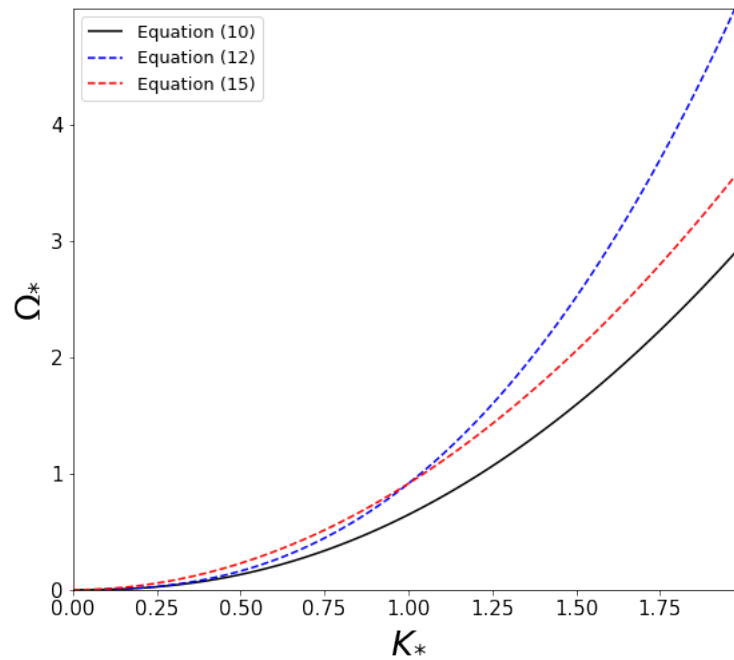


Figure 3. Comparison of the leading-order approximation (10) (solid black line) with one-term expansion (12) for $K_* \ll 1$ (dashed blue line) and one-term expansion (15) for $K_* \gg 1$ (dashed red line).

4. Asymptotic Models

4.1. Scaling

Below, for the first time, we proceed with the asymptotic dimension reduction for the dynamic equations in linear elasticity using the small ratio of densities r , typical for light fluid loading, as the main small parameter. The developed procedure amends the approach delivered in the recent paper [17].

First, scale the independent variables specified in the previous section by

$$t = T\tau, \quad x_1 = L\zeta, \quad x_3 = \begin{cases} Lr\zeta, & \text{if } |x_3| < h, \\ L\gamma, & \text{otherwise,} \end{cases} \tag{18}$$

where for the sake of simplicity $L = h/r$, ($L \gg h$) is a typical wavelength and $T = \frac{h}{r^2c_2}$, ($T \gg h/c_2$), which is motivated by the relation $\omega h/c_2 \sim (kh)^{5/2}$ between angular frequency ω and wave number k for a fluid-borne bending wave; see [28] as well as Formula (8) in Section 3.

Next, introduce the dimensionless stresses, displacements, and fluid potential setting

$$\begin{aligned} \sigma_{11} &= Er\sigma_{11}^*, & \sigma_{22} &= Er\sigma_{22}^*, & \sigma_{31} &= Er^2\sigma_{31}^*, & \sigma_{33} &= Er^3\sigma_{33}^*, \\ v_1 &= hv_1^*, & v_3 &= \frac{h}{r}v_3^*, & \varphi &= \frac{h^2}{r^2}\varphi^*. \end{aligned} \tag{19}$$

The starred quantities above are assumed to be of order unity. Hence, Equations (1) and (2) can be written in the following dimensionless form

$$\begin{aligned} \frac{\partial \sigma_{31}^*}{\partial \zeta} &= -\frac{\partial \sigma_{11}^*}{\partial \zeta} + \frac{1}{2(1+\nu)}r^2\frac{\partial^2 v_1^*}{\partial \tau^2}, \\ \frac{\partial \sigma_{33}^*}{\partial \zeta} &= -\frac{\partial \sigma_{31}^*}{\partial \zeta} + \frac{1}{2(1+\nu)}\frac{\partial^2 v_3^*}{\partial \tau^2}, \end{aligned} \tag{20}$$

and

$$\begin{aligned}
 \sigma_{11}^* &= \frac{1}{1-\nu^2} \frac{\partial v_1^*}{\partial \zeta} + \frac{\nu}{1-\nu} r^2 \sigma_{33}^*, \\
 \sigma_{22}^* &= \frac{\nu}{1-\nu^2} \frac{\partial v_1^*}{\partial \zeta} + \frac{\nu}{1-\nu} r^2 \sigma_{33}^*, \\
 \frac{\partial v_3^*}{\partial \zeta} &= r^4 \sigma_{33}^* - \nu r^2 (\sigma_{11}^* + \sigma_{22}^*), \\
 \frac{\partial v_1^*}{\partial \zeta} &= -\frac{\partial v_3^*}{\partial \zeta} + 2(1+\nu) r^2 \sigma_{31}^*.
 \end{aligned}
 \tag{21}$$

In addition, the dimensionless form of relations (3) and (4) becomes

$$\frac{\partial^2 \varphi^*}{\partial \zeta^2} + \frac{\partial^2 \varphi^*}{\partial \gamma^2} - r^2 \delta^2 \frac{\partial^2 \varphi^*}{\partial \tau^2} = 0,
 \tag{22}$$

and

$$\begin{aligned}
 \sigma_{31}^* \Big|_{\zeta=\pm 1} &= 0, & \sigma_{33}^* \Big|_{\zeta=\pm 1} &= \frac{1}{2(1+\nu)} \frac{\partial^2 \varphi^*}{\partial \tau^2} \Big|_{\gamma=\pm r}, \\
 \frac{\partial \varphi^*}{\partial \gamma} \Big|_{\gamma=\pm r} &= v_3^* \Big|_{\zeta=\pm 1}.
 \end{aligned}
 \tag{23}$$

Next, expand the starred displacement and stress components as well as the fluid displacement potential in an asymptotic series as

$$\begin{aligned}
 v_1^* &= v_1^{(0)} + r^2 v_1^{(1)} + r^4 v_1^{(2)} + \dots \\
 v_3^* &= v_3^{(0)} + r^2 v_3^{(1)} + r^4 v_3^{(2)} + \dots \\
 \sigma_{11}^* &= \sigma_{11}^{(0)} + r^2 \sigma_{11}^{(1)} + r^4 \sigma_{11}^{(2)} + \dots \\
 \sigma_{22}^* &= \sigma_{22}^{(0)} + r^2 \sigma_{22}^{(1)} + r^4 \sigma_{22}^{(2)} + \dots \\
 \sigma_{33}^* &= \sigma_{33}^{(0)} + r^2 \sigma_{33}^{(1)} + r^4 \sigma_{33}^{(2)} + \dots \\
 \sigma_{31}^* &= \sigma_{31}^{(0)} + r^2 \sigma_{31}^{(1)} + r^4 \sigma_{31}^{(2)} + \dots \\
 \varphi^* &= \varphi^{(0)} + r^2 \varphi^{(1)} + r^4 \varphi^{(2)} + \dots
 \end{aligned}
 \tag{24}$$

leading to shortened forms of the original plane-strain problem in hydro-elasticity.

In what follows, we restrict ourselves to antisymmetric motion about the midplane $x_3 = 0$. In this case, due to the symmetry of the problem, only the interfacial conditions along the upper face $x_3 = h$ are considered.

4.2. Leading-Order Approximation

Here, we focus on the leading-order approximation of the problem formulated in the previous subsection, retaining only the terms with the suffix (0) in the asymptotic series (24). Firstly, integrating (21)₃–(21)₄ along the thickness variable ζ , we obtain, respectively,

$$v_3^{(0)} = V_3^{(0)}(\zeta, \tau) \quad \text{and} \quad v_1^{(0)} = -\zeta \frac{\partial V_3^{(0)}}{\partial \zeta}.
 \tag{25}$$

Upon substituting the displacements (25) into (21)₁–(21)₂, we obtain

$$\sigma_{11}^{(0)} = -\zeta \frac{1}{1-\nu^2} \frac{\partial^2 V_3^{(0)}}{\partial \xi^2} \quad \text{and} \quad \sigma_{22}^{(0)} = -\zeta \frac{\nu}{1-\nu^2} \frac{\partial^2 V_3^{(0)}}{\partial \xi^2}. \tag{26}$$

Next, integrating (20)₁ along ζ , taking into account (25) and (26), leads to

$$\sigma_{31}^{(0)} = \zeta^2 \frac{1}{2(1-\nu^2)} \frac{\partial^3 V_3^{(0)}}{\partial \xi^3} + C^{(0)}(\zeta, \tau), \tag{27}$$

where $C^{(0)}$ is an arbitrary function. Finally, inserting (25)–(27) into (20)₂ and integrating along ζ yields

$$\sigma_{33}^{(0)} = -\zeta^3 \frac{1}{6(1-\nu^2)} \frac{\partial^4 V_3^{(0)}}{\partial \xi^4} - \zeta \frac{\partial C^{(0)}}{\partial \xi} + \zeta \frac{1}{2(1+\nu)} \frac{\partial^2 V_3^{(0)}}{\partial \tau^2}. \tag{28}$$

Furthermore, the fluid potential at the leading order can be obtained by inserting (24)₇ into (22), arriving at the Laplace equation

$$\frac{\partial^2 \varphi^{(0)}}{\partial \xi^2} + \frac{\partial^2 \varphi^{(0)}}{\partial \gamma^2} = 0, \tag{29}$$

which governs incompressible fluid. On the other hand, inserting (24) into (23), leads to the interfacial conditions

$$\sigma_{31}^{(0)} \Big|_{\zeta=1} = 0, \quad \sigma_{33}^{(0)} \Big|_{\zeta=1} = \frac{1}{2(1+\nu)} \frac{\partial^2 \varphi^{(0)}}{\partial \tau^2} \Big|_{\gamma=r}, \quad \frac{\partial \varphi^{(0)}}{\partial \gamma} \Big|_{\gamma=r} = v_3^{(0)}. \tag{30}$$

By applying (30)₁ and (30)₂ to (27) and (28), respectively, we arrive at

$$C^{(0)} = -\frac{1}{2(1-\nu^2)} \frac{\partial^3 V_3^{(0)}}{\partial \xi^3}, \tag{31}$$

and

$$\frac{2}{3(1-\nu)} \frac{\partial^4 V_3^{(0)}}{\partial \xi^4} + \frac{\partial^2 V_3^{(0)}}{\partial \tau^2} - \frac{\partial^2 \varphi^{(0)}}{\partial \tau^2} \Big|_{\gamma=r} = 0. \tag{32}$$

The derived equation corresponds to a fluid-loaded Kirchhoff plate, which is similar to the one derived at the first (not leading) order in [17]. It is worth noting that the leading-order approximation in [17], dealing with a non-contrast case, does not contain transverse plate inertia, given by the second term in (32).

4.3. First-Order Approximation

In this subsection, the first-order approximation is derived, also retaining the terms with the suffix (1) in the asymptotic series (24). The procedure is essentially the same as in the previous subsection; hence, some of the intermediate computations are omitted. Now, we have

$$\frac{\partial^2 \varphi^{(1)}}{\partial \xi^2} + \frac{\partial^2 \varphi^{(1)}}{\partial \gamma^2} - \delta^2 \frac{\partial^2 \varphi^{(0)}}{\partial \tau^2} = 0, \tag{33}$$

and

$$\begin{aligned}
 v_3^{(1)} &= \zeta^2 \frac{\nu}{2(1-\nu)} \frac{\partial^2 V_3^{(0)}}{\partial \xi^2} + V_3^{(1)}(\zeta, \tau), \\
 v_1^{(1)} &= \frac{1}{6(1-\nu)} ((2-\nu)\zeta^3 - 6\zeta) \frac{\partial^3 V_3^{(0)}}{\partial \xi^3} - \zeta \frac{\partial V_3^{(1)}}{\partial \xi}, \\
 \sigma_{11}^{(1)} &= \frac{1}{6(1-\nu)(1-\nu^2)} (2(1-\nu)\zeta^3 + 3(\nu-2)\zeta) \frac{\partial^4 V_3^{(0)}}{\partial \xi^4} \\
 &\quad - \zeta \frac{1}{1-\nu^2} \frac{\partial^2 V_3^{(1)}}{\partial \xi^2} + \zeta \frac{\nu}{2(1-\nu^2)} \frac{\partial^2 V_3^{(0)}}{\partial \tau^2}, \\
 \sigma_{22}^{(1)} &= \frac{\nu}{6(1-\nu)(1-\nu^2)} ((1-\nu)\zeta^3 - 3\zeta) \frac{\partial^4 V_3^{(0)}}{\partial \xi^4} \\
 &\quad - \zeta \frac{\nu}{1-\nu^2} \frac{\partial^2 V_3^{(1)}}{\partial \xi^2} + \zeta \frac{\nu}{2(1-\nu^2)} \frac{\partial^2 V_3^{(0)}}{\partial \tau^2}, \\
 \sigma_{31}^{(1)} &= -\frac{1}{12(1-\nu)(1-\nu^2)} ((1-\nu)\zeta^4 + 3(\nu-2)\zeta^2) \frac{\partial^5 V_3^{(0)}}{\partial \xi^5} \\
 &\quad + \zeta^2 \frac{1}{2(1-\nu^2)} \frac{\partial^3 V_3^{(1)}}{\partial \xi^3} - \zeta^2 \frac{1}{4(1-\nu^2)} \frac{\partial^3 V_3^{(0)}}{\partial \xi \partial \tau^2} + C^{(1)}(\zeta, \tau), \\
 \sigma_{33}^{(1)} &= \frac{1}{60(1-\nu)(1-\nu^2)} ((1-\nu)\zeta^5 + 5(\nu-2)\zeta^3) \frac{\partial^6 V_3^{(0)}}{\partial \xi^6} \\
 &\quad - \zeta^3 \frac{1}{6(1-\nu^2)} \frac{\partial^4 V_3^{(1)}}{\partial \xi^4} + \zeta^3 \frac{1}{12(1-\nu)} \frac{\partial^4 V_3^{(0)}}{\partial \xi^2 \partial \tau^2} \\
 &\quad - \zeta \frac{\partial C^{(1)}}{\partial \xi} + \zeta \frac{1}{2(1+\nu)} \frac{\partial^2 V_3^{(1)}}{\partial \tau^2},
 \end{aligned} \tag{34}$$

where $C^{(1)}$ is an arbitrary function; the interfacial conditions are given by

$$\sigma_{31}^{(1)} \Big|_{\zeta=1} = 0, \quad \sigma_{33}^{(1)} \Big|_{\zeta=1} = \frac{1}{2(1+\nu)} \frac{\partial^2 \varphi^{(1)}}{\partial \tau^2} \Big|_{\gamma=r}, \quad \frac{\partial \varphi^{(1)}}{\partial \gamma} \Big|_{\gamma=r} = v_3^{(1)}. \tag{35}$$

Furthermore, applying (35)₁ and (35)₂ to (34)₅ and (34)₆, respectively, we obtain

$$C^{(1)} = \frac{2\nu-5}{12(1-\nu)(1-\nu^2)} \frac{\partial^5 V_3^{(0)}}{\partial \xi^5} - \frac{1}{2(1-\nu^2)} \frac{\partial^3 V_3^{(1)}}{\partial \xi^3} + \frac{1}{4(1-\nu^2)} \frac{\partial^3 V_3^{(0)}}{\partial \xi \partial \tau^2}, \tag{36}$$

and

$$\begin{aligned}
 &\frac{2}{3(1-\nu)} \frac{\partial^4 V_3^{(1)}}{\partial \xi^4} + \frac{\partial^2}{\partial \tau^2} \left(V_3^{(1)} + \frac{7\nu-17}{15(1-\nu)} \frac{\partial^2 V_3^{(0)}}{\partial \xi^2} \right) \\
 &+ \frac{\partial^2}{\partial \tau^2} \left(\frac{8-3\nu}{10(1-\nu)} \frac{\partial^2 \varphi^{(0)}}{\partial \xi^2} - \varphi^{(1)} \right) \Big|_{\gamma=r} = 0.
 \end{aligned} \tag{37}$$

The comparison of (37) with the refined equation for an elastic plate in the absence of fluid but subject to prescribed mechanical loading, as articulated in [18,29], manifests that the two equations are in complete agreement. At this order, the terms involving transverse shear deformation, plate rotatory inertia, and fluid compressibility have to be kept, unlike in [17], where these terms did not appear until the third-order approximation.

4.4. Asymptotically Consistent Equations

This subsection is concerned with the formulation of asymptotic models, i.e., shortened equations of motion for a thin elastic plate immersed in fluid together with the impenetrability conditions along the interfaces, originating from the results entrenched in the previous section. At the leading order, we obtain from (29), (30)₃ and (32)

$$\frac{2}{3(1-\nu)} \frac{\partial^4 v_3^*}{\partial \xi^4} + \frac{\partial^2 v_3^*}{\partial \tau^2} - \frac{\partial^2 \varphi^*}{\partial \tau^2} \Big|_{\gamma=r} = 0, \tag{38}$$

$$\frac{\partial^2 \varphi^*}{\partial \xi^2} + \frac{\partial^2 \varphi^*}{\partial \gamma^2} = 0, \tag{39}$$

and

$$\frac{\partial \varphi^*}{\partial \gamma} \Big|_{\gamma=r} = v_3^*, \tag{40}$$

where $v_3^*(\xi, 0, \tau) = V_3^{(0)}(\xi, \tau)$ and $\varphi^*(\xi, \gamma, \tau) = \varphi^{(0)}(\xi, \gamma, \tau)$. In original variables, Equations (38)–(40) become

$$\frac{Eh^3}{3(1-\nu^2)} \frac{\partial^4 v_3}{\partial x_1^4} + \rho h \frac{\partial^2 v_3}{\partial t^2} - \rho_0 \frac{\partial^2 \varphi}{\partial t^2} \Big|_{x_3=h} = 0, \tag{41}$$

$$\frac{\partial^2 \varphi}{\partial x_1^2} + \frac{\partial^2 \varphi}{\partial x_3^2} = 0, \tag{42}$$

and

$$\frac{\partial \varphi}{\partial x_3} \Big|_{x_3=h} = v_3. \tag{43}$$

It is important to note that here and for the rest of this section, v_3 (the transverse displacement) is taken at the midplane $x_3 = 0$, i.e., $v_3 = v_3(x_1, 0, t)$. Hence, Equations (41)–(43) correspond to the traditional setup of a Kirchhoff plate submerged in incompressible fluid.

Next, consider the sum of Equations (32) and (37), multiplied by the small parameter r^2 , to obtain

$$\begin{aligned} & \frac{2}{3(1-\nu)} \frac{\partial^4}{\partial \xi^4} \left(V_3^{(0)} + r^2 V_3^{(1)} \right) + \frac{\partial^2}{\partial \tau^2} \left(V_3^{(0)} + r^2 V_3^{(1)} \right) \\ & - \frac{\partial^2}{\partial \tau^2} \left(\varphi^{(0)} + r^2 \varphi^{(1)} \right) \Big|_{\gamma=r} + r^2 \frac{7\nu - 17}{15(1-\nu)} \frac{\partial^4}{\partial \xi^2 \partial \tau^2} \left(V_3^{(0)} + r^2 V_3^{(1)} \right) \\ & + r^2 \frac{8 - 3\nu}{10(1-\nu)} \frac{\partial^4}{\partial \xi^2 \partial \tau^2} \left(\varphi^{(0)} + r^2 \varphi^{(1)} \right) \Big|_{\gamma=r} + O(r^4) = 0. \end{aligned} \tag{44}$$

In a similar manner, we have from Equations (29), (33), (30)₃ and (35)₃, respectively

$$\frac{\partial^2}{\partial \xi^2} \left(\varphi^{(0)} + r^2 \varphi^{(1)} \right) + \frac{\partial^2}{\partial \gamma^2} \left(\varphi^{(0)} + r^2 \varphi^{(1)} \right) - r^2 \delta^2 \frac{\partial^2}{\partial \tau^2} \left(\varphi^{(0)} + r^2 \varphi^{(1)} \right) + O(r^4) = 0, \tag{45}$$

and

$$\frac{\partial}{\partial \gamma} \left(\varphi^{(0)} + r^2 \varphi^{(1)} \right) \Big|_{\gamma=r} = V_3^{(0)} + r^2 V_3^{(1)} + r^2 \frac{\nu}{2(1-\nu)} \frac{\partial^2}{\partial \xi^2} \left(V_3^{(0)} + r^2 V_3^{(1)} \right) + O(r^4). \tag{46}$$

By neglecting terms of $O(r^4)$, Formulas (44)–(46) can be rewritten as

$$\begin{aligned} \frac{2}{3(1-\nu)} \frac{\partial^4 v_3^*}{\partial \xi^4} + \frac{\partial^2 v_3^*}{\partial \tau^2} - \frac{\partial^2 \varphi^*}{\partial \tau^2} \Big|_{\gamma=r} + r^2 \frac{7\nu - 17}{15(1-\nu)} \frac{\partial^4 v_3^*}{\partial \xi^2 \partial \tau^2} \\ + r^2 \frac{8 - 3\nu}{10(1-\nu)} \frac{\partial^4 \varphi^*}{\partial \xi^2 \partial \tau^2} \Big|_{\gamma=r} = 0, \end{aligned} \tag{47}$$

and

$$\frac{\partial^2 \varphi^*}{\partial \xi^2} + \frac{\partial^2 \varphi^*}{\partial \gamma^2} - r^2 \delta^2 \frac{\partial^2 \varphi^*}{\partial \tau^2} = 0, \tag{48}$$

with

$$\frac{\partial \varphi^*}{\partial \gamma} \Big|_{\gamma=r} = v_3^* + r^2 \frac{\nu}{2(1-\nu)} \frac{\partial^2 v_3^*}{\partial \xi^2}, \tag{49}$$

where $v_3^* = V_3^{(0)} + r^2 V_3^{(1)}$ and $\varphi^* = \varphi^{(0)} + r^2 \varphi^{(1)}$. In terms of original variables, Equations (47) and (49) take the form

$$\begin{aligned} \frac{Eh^3}{3(1-\nu^2)} \frac{\partial^4 v_3}{\partial x_1^4} + \rho h \left(1 + h^2 \frac{7\nu - 17}{15(1-\nu)} \frac{\partial^2}{\partial x_1^2} \right) \frac{\partial^2 v_3}{\partial t^2} \\ - \rho_0 \left(1 - h^2 \frac{8 - 3\nu}{10(1-\nu)} \frac{\partial^2}{\partial x_1^2} \right) \frac{\partial^2 \varphi}{\partial t^2} \Big|_{x_3=h} = 0, \end{aligned} \tag{50}$$

with

$$\frac{\partial \varphi}{\partial x_3} \Big|_{x_3=h} = \left(1 + \frac{\nu h^2}{2(1-\nu)} \frac{\partial^2}{\partial x_1^2} \right) v_3, \tag{51}$$

together with Equation (3), governing the compressible fluid motion (Equation (48) in original variables).

Hence, Equations (3), (50) and (51) correspond to the first-order asymptotic model, which incorporates three corrections, including transverse shear deformation, plate rotation inertia, and fluid compressibility. We re-iterate that the aforementioned first-order model coincides with the third-order model derived in [17], which does not assume that r is a small parameter.

4.5. Comparison of Dispersion Relations

The focus of this subsection is to derive the dispersion relations corresponding to the approximate formulations established in the previous Section 4.4 and to establish the link between these and the leading- and first-order approximations obtained in Section 3.

Begin with the travelling wave solution of the leading-order problem (41)–(43), setting

$$\begin{aligned} v_3 &= e^{i(kx_1 - \omega t)}, \\ \varphi &= -\frac{1}{k} e^{-k(x_3 - h) + i(kx_1 - \omega t)}, \end{aligned} \tag{52}$$

Upon substituting (52) into the aforementioned formulae, we arrive at the dispersion relation

$$\Omega^2 = \frac{2}{3(1-\nu)} \frac{K^5}{r + K'} \tag{53}$$

where K and Ω are dimensionless wavenumber and frequency, respectively, defined by (7).

Next, we set

$$v_3(x_1, 0) = e^{i(kx_1 - \omega t)},$$

$$\varphi = - \left(k^2 - \frac{\omega^2}{c_0^2} \right)^{-\frac{1}{2}} \left(1 - \frac{\nu h^2 k^2}{2(1-\nu)} \right) e^{- \left(k^2 - \frac{\omega^2}{c_0^2} \right)^{\frac{1}{2}} (x_3 - h) + i(kx_1 - \omega t)}, \tag{54}$$

in Equations (3), (50) and (51), resulting in the dispersion relation for the first-order model, given by

$$\Omega^2 \left(60(1-\nu)^2 H + 3r(3\nu-8)(2(\nu-1) + \nu K^2) K^2 + 4(1-\nu)(17-7\nu) K^2 H - 30r(1-\nu)(2(\nu-1) + \nu K^2) \right) = 40(1-\nu) K^4 H, \tag{55}$$

where H is defined in (6).

It can be easily verified that substituting (8) into (53) leads to the leading-order approximation given by Equation (10). On the other hand, when substituting (8) into (55) and expanding for small r and retaining of two terms leads to the first-order approximation given by (11). This clearly demonstrates the link between the asymptotic models and the approximate equations given in Section 3. The comparison of (11) and (55) is displayed in Figure 4, showing excellent agreement.

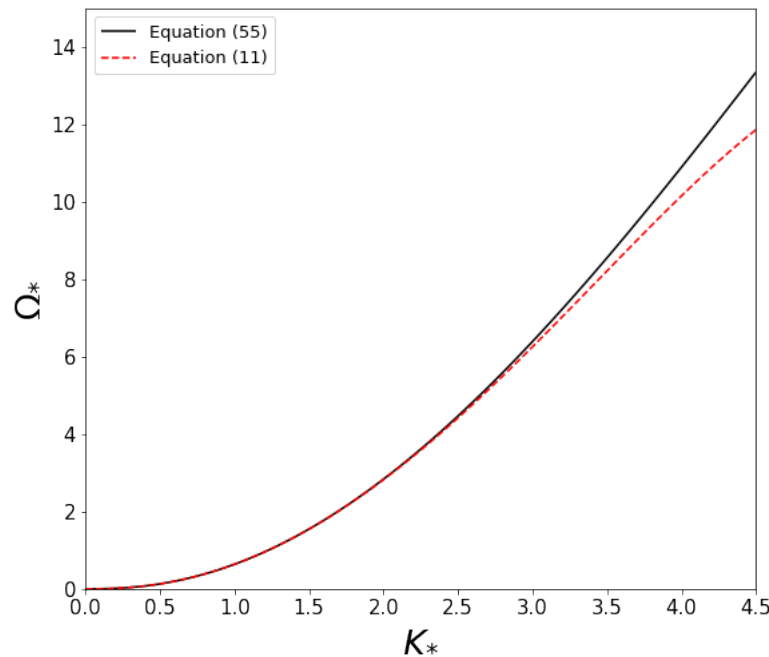


Figure 4. Comparison of the first-order dispersion relation (55) (solid black line) with the first-order approximation (11) (dashed red line) for the same parameters as in Section 3.

5. Concluding Remarks

In this paper, the two-step asymptotic analysis of light fluid loading has been developed. The first step is concerned with the derivation of the leading- and first-order approximations of the full dispersion relation. The second step is oriented towards the leading- and first-order asymptotic models, including the equations of motion and impenetrability condition. The presence of a small parameter, expressing light fluid loading, assumes the plate inertia to be incorporated into the leading-order model. At the same

time, transverse shear deformation, plate rotation inertia, fluid compressibility, and other similar corrections appear at the next order.

The model problem considered in this paper can be readily extended to more elaborated setups, including one-side contact, fluid-loaded thin elastic shells, and radiation and scattering by submerged structures.

Author Contributions: S.S.: computation, investigation, methodology, problem statement, writing—original draft, writing—review and editing. L.P.: conceptualization, methodology, problem statement, supervision, writing—review and editing. All authors have read and agreed to the published version of the manuscript.

Funding: This research received no external funding.

Data Availability Statement: Data are contained within the article.

Acknowledgments: Fruitful discussions with J. Kaplunov are greatly acknowledged.

Conflicts of Interest: The authors declare no conflicts of interest.

References

1. Rayleigh, J.W.S.B. *The Theory of Sound*; Macmillan: New York, NY, USA, 1896; Volume 2.
2. Crighton, D. The 1988 Rayleigh medal lecture: Fluid loading—The interaction between sound and vibration. *J. Sound Vib.* **1989**, *133*, 1–27. [\[CrossRef\]](#)
3. Crighton, D.G.; Dowling, A.P.; Ffowcs-Williams, J.; Heckl, M.; Leppington, F.; Bartram, J.F. *Modern Methods in Analytical Acoustics Lecture Notes*; Springer: London, UK, 1992.
4. Junger, M.C.; Feit, D. *Sound, Structures, and Their Interaction*; MIT Press: Cambridge, MA, USA, 1986; Volume 225.
5. Norris, A.N.; Rebinsky, D.A. Acoustic coupling to membrane waves on elastic shells. *J. Acoust. Soc. Am.* **1994**, *95*, 1809–1829. [\[CrossRef\]](#)
6. Blonigen, F.J.; Marston, P.L. Leaky helical flexural wave scattering contributions from tilted cylindrical shells: Ray theory and wave-vector anisotropy. *J. Acoust. Soc. Am.* **2001**, *110*, 1764–1769. [\[CrossRef\]](#)
7. Caresta, M.; Kessissoglou, N.J. Structural and acoustic responses of a fluid-loaded cylindrical hull with structural discontinuities. *Appl. Acoust.* **2009**, *70*, 954–963. [\[CrossRef\]](#)
8. Titovich, A.S.; Norris, A.N. Acoustic scattering from an infinitely long cylindrical shell with an internal mass attached by multiple axisymmetrically distributed stiffeners. *J. Sound Vib.* **2015**, *338*, 134–153. [\[CrossRef\]](#)
9. Ruotolo, R. A comparison of some thin shell theories used for the dynamic analysis of stiffened cylinders. *J. Sound Vib.* **2001**, *243*, 847–860. [\[CrossRef\]](#)
10. Homm, A.; Ehrlich, J.; Peine, H.; Wiesner, H. Experimental and numerical investigation of a complex submerged structure. Part I: Modal analysis. *Acta Acust. United Acust.* **2003**, *89*, 61–70.
11. Forrest, J.A. Measured dynamics of a thin cylindrical shell subject to axial excitation. In Proceedings of the Acoustics 2005, Busselton, WA, Australia, 9–11 November 2005; pp. 9–11.
12. Slepyan, L.; Sorokin, S. Analysis of structural-acoustic coupling problems by a two-level boundary integral method: Part 1: A general formulation and test problems. *J. Sound Vib.* **1995**, *184*, 195–211. [\[CrossRef\]](#)
13. Cole, J.E., III. Vibrations of a framed cylindrical shell submerged in and filled with acoustic fluids: Spectral solution. *Comput. Struct.* **1997**, *65*, 385–393. [\[CrossRef\]](#)
14. Liu, C.H.; Chen, P.T. Numerical analysis of immersed finite cylindrical shells using a coupled BEM/FEM and spatial spectrum approach. *Appl. Acoust.* **2009**, *70*, 256–266. [\[CrossRef\]](#)
15. Johansson, M.; Folkow, P.D.; Hägglund, A.; Olsson, P. Approximate boundary conditions for a fluid-loaded elastic plate. *J. Acoust. Soc. Am.* **2005**, *118*, 3436–3446. [\[CrossRef\]](#)
16. Belov, A.; Kaplunov, J.; Nolde, E. A refined asymptotic model of fluid-structure interaction in scattering by elastic shells. *Flow Turbul. Combust.* **1998**, *61*, 255–267. [\[CrossRef\]](#)
17. Kaplunov, J.; Prikazchikova, L.; Shamsi, S. A hierarchy of asymptotic models for a fluid-loaded elastic layer. *Math. Mech. Solids* **2023**, *29*, 560–576. [\[CrossRef\]](#)
18. Kaplunov, J.D.; Kossovitch, L.Y.; Nolde, E. *Dynamics of Thin Walled Elastic Bodies*; Academic Press: Cambridge, MA, USA, 1998.
19. Talmant, M.; Überall, H.; Miller, R.D.; Werby, M.F.; Dickey, J. Lamb waves and fluid-borne waves on water-loaded, air-filled thin spherical shells. *J. Acoust. Soc. Am.* **1989**, *86*, 278–289. [\[CrossRef\]](#)
20. Yücel, H.; Ege, N.; Erbaş, B.; Kaplunov, J. A revisit to the plane problem for low-frequency acoustic scattering by an elastic cylindrical shell. *Math. Mech. Solids* **2024**. [\[CrossRef\]](#)
21. Craster, R. The light fluid loading limit for fluid/solid interactions. *Eur. J. Appl. Math.* **1997**, *8*, 485–505. [\[CrossRef\]](#)
22. Sorokin, S.V. Analysis of wave propagation in sandwich plates with and without heavy fluid loading. *J. Sound Vib.* **2004**, *271*, 1039–1062. [\[CrossRef\]](#)

23. Sorokin, S.V. Vibrations of and sound radiation from sandwich plates in heavy fluid loading conditions. *Compos. Struct.* **2000**, *48*, 219–230. [[CrossRef](#)]
24. Chapman, C.J.; Sorokin, S.V. The forced vibration of an elastic plate under significant fluid loading. *J. Sound Vib.* **2005**, *281*, 719–741. [[CrossRef](#)]
25. Kaplunov, J.; Markushevich, D. Plane vibrations and radiation of an elastic layer lying on a liquid half-space. *Wave Motion* **1993**, *17*, 199–211. [[CrossRef](#)]
26. Howe, M.S. *Acoustics of Fluid-Structure Interactions*; Cambridge University Press: Cambridge, UK, 1998.
27. Nakayama, Y. *Introduction to Fluid Mechanics*; Butterworth-Heinemann: Oxford, UK, 2018.
28. Kaplunov, J.; Prikazchikova, L.; Shamsi, S. Dispersion of the Bending Wave in a Fluid-loaded Elastic Layer. In *Advances in Solid and Fracture Mechanics: A Liber Amicorum to Celebrate the Birthday of Nikita Morozov*; Springer: Berlin/Heidelberg, Germany, 2022; pp. 127–134.
29. Goldenveizer, A.; Kaplunov, J.; Nolde, E. On Timoshenko-Reissner type theories of plates and shells. *Int. J. Solids Struct.* **1993**, *30*, 675–694. [[CrossRef](#)]

Disclaimer/Publisher’s Note: The statements, opinions and data contained in all publications are solely those of the individual author(s) and contributor(s) and not of MDPI and/or the editor(s). MDPI and/or the editor(s) disclaim responsibility for any injury to people or property resulting from any ideas, methods, instructions or products referred to in the content.